Physica B: Condensed Matter 545 (2018) 159–166

Contents lists available at ScienceDirect

Physica B: Condensed Matter

journal homepage: www.elsevier.com/locate/physb

Linear giant Stark effect in WSe_2 nanoribbons

Mohsen Shahbazi

Department of Physics, Factualy of Science, University of Zanjan, Zanjan 45371-38791, Iran

ARTICLE INFO

Keywords:
WSe_2 nanoribbon
Tight binding
Electric field
Stark effect
Spin polarization
Exchange interaction

ABSTRACT

In this paper the electronic properties of WSe_2 nanoribbons is theoretically and numerically investigated by using six-band tight-binding (TB) model. Zigzag and armchair models of WSe_2 nanoribbon show semiconducting and metallic phases, respectively. Effect of external electric field on the electronic properties of WSe_2 via solving the Laplace's equation is also studied. A semiconductor-metal phase transition is observed for armchair structure by 2.1 $\frac{V}{w}$ of applied transverse electric field, where w is the width of the ribbon. A linear giant Stark effect is also occurred in both armchair and zigzag WSe_2 nanoribbons by variations of applied transverse electric field. Moreover, we investigate electronic transport of armchair WSe_2 nanoribbon putting on a ferromagnetic EuS substrate using nonequilibrium Green's function method. Spin polarization is occurred by effect of an exchange field of 0.2 eV, induced by a ferromagnetic EuS substrate.

1. Introduction

Two dimensional (2D) materials similar to graphene and monolayer of the transition metal dichalcogenides (TMDs) that recently have been introduced, are in the attention of scientists due to their exciting electronic properties. These materials have high carrier mobility [1] and have very high flexibility under strain so that their electronic properties could be tuned by strain engineering [2,3]. Notice that the intrinsic energy band gap of TMDs and graphene is different [4]. Moreover, TMDs, similar to MoS_2, could possess lattice defects that can be helpful to tune their electronic properties by defect management [5]. Generally, TMDs are marked with MX_2, where M stands for Mo or W, and also X stands for Te, S and Se. Recently electronic devices such as Field Effect Transistors (FET), sensors [6], and optical transistors [7] have been introduced based on TMDs. By thinned down from bulk to monolayer in TMDs, the inverse symmetry is broken [8]. There is an indirect energy gap of 0.94 eV for bulk WSe_2, while a direct band gap of 1.61 eV in its monolayer is observed by Kumar et al. [4]. In WSe_2 monolayer the Tungsten layer stands between two layers of Selenium via covalent bonds [9]. By means of external perturbations, it is possible to control the electronic and optical properties of a monolayers of WSe_2. For example, it is possible to control the valley degree of freedoms by applying external magnetic fields [10]. Valley Zeeman effect has experimentally been observed by applying external magnetic field in WSe_2 monolayer [11]. The giant Zeeman-type spin polarization can also be tuned by exerting external electric field in WSe_2 monolayer [12].

In this paper, both tight binding and Green's function methods have been utilized to investigate electronic and transport properties of WSe_2 nanoribbons. Slater-Koster approach have also been employed to calculate hopping energies in a monolayer of WSe_2 [13]. Notice that due to the presence of horizontal mirror symmetry for monolayer of WSe_2, a reduced six-band Hamiltonian is utilized in this work. Furthermore, we evaluate the variations of electronic properties of zigzag and armchair WSe_2 nanoribbons in the presence of transverse electric field. Linear giant Stark effect is also occurred by varying the external electric field in both zigzag and armchair WSe_2 nanoribbons. Moreover, effect of an induced exchange field via a magnetic EuS substrate is perused.

This paper is organized as follow. In Sec. 2, tight binding model that is utilized to calculate the energy band structure for both nanosheet and nanoribbon is explained. In Sec. 3, the Green's function approach is described to calculate the conductance and spin polarization. In Sec. 4, we investigate effect of external electric field and also an induced exchange field on the initial tight binding Hamiltonian of WSe_2 single-layer. In Sec. 5, we present our main results, including energy dispersion in the systems, energy dispersion in presence of external electric field, variations of energy band gap as a function of external electric fields, and eventually conductance and spin polarization in the presence of an induced exchange field by ferromagnetic EuS substrate. Finally, we summarize our main results in Sec. 6.

2. Theory and methodology

To determine electronic state of crystalline materials different techniques can be used. Tight binding, using the well-known Bloch theory, is a powerful technique for this purpose. That is related to the

E-mail address: mohsenshahbazi1984@yahoo.com.

https://doi.org/10.1016/j.physb.2018.06.004
Received 9 January 2018; Received in revised form 22 May 2018; Accepted 3 June 2018

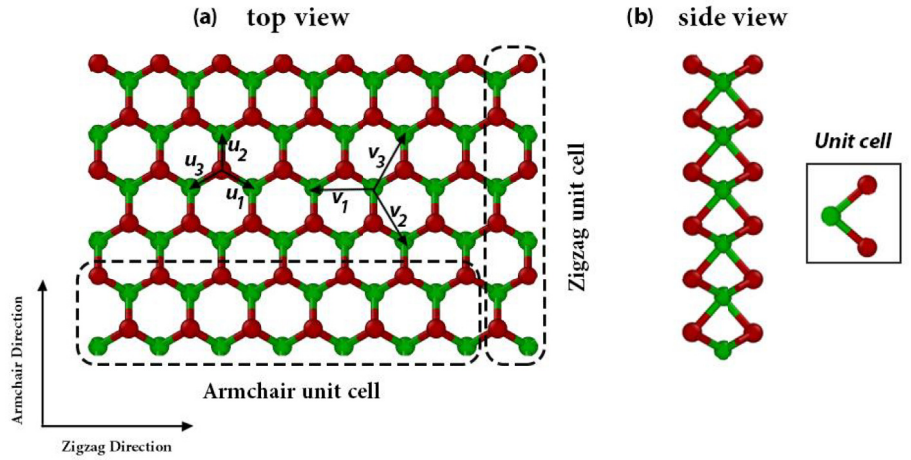

Fig. 1. (a) Top view and (b) side view of a WSe_2 monolayer. Green and red circles indicate W and Se atoms respectively. u_i and v_i refer to nearest and next nearest neighbors, respectively. (For interpretation of the references to colour in this figure legend, the reader is referred to the Web version of this article.)

Table 1
Tight binding parameters of WSe_2 monolayer. All energies are in eV unite.

Crystal Fields	f_0	− 0.935
	f_2	− 2.321
	f_p	− 5.629
	f_z	− 6.759
W− Se	$V_{pd\sigma}$	5.803
	$V_{pd\pi}$	− 1.081
W− W	$V_{dd\sigma}$	− 1.129
	$V_{dd\pi}$	0.094
	$V_{dd\delta}$	0.317
Se − Se	$V_{pp\sigma}$	1.530
	$V_{pp\pi}$	− 0.123

linear combination of atomic orbitals (LCAO). Single-layer of WSe_2 has honeycomb lattice structure in top view (Fig. 1(a)) and three layers in side view, Fig. 1(b). A unit cell is considered including one Tungsten atom in the middle and two Selenium atoms in top and bottom, see Fig. 1(b). Hence, five d orbitals of Tungsten and three p orbitals of each of the Selenium atoms form the Hilbert space. Therefore, this Hilbert space can be read as $\left(d_{xy}, d_{yz}, d_{xz}, d_{x^2-y^2}, d_{3z^2-r^2}, p_x^t, p_y^t, p_z^t, p_x^b, p_y^b, p_z^b\right)$ which build eleven-band tight binding model. A unitary transformation can be utilized due to the horizontal reflection symmetry proportional to z-axis so that this 11×11 matrix of Hamiltonian can be divided to even and odd subspace. The even subspace of the P orbitals can be written as following:

$$P_x^S = \frac{1}{\sqrt{2}}(p_x^t + p_x^b), \tag{1}$$

$$P_y^S = \frac{1}{\sqrt{2}}\left(p_y^t + p_y^b\right), \tag{2}$$

$$P_z^A = \frac{1}{\sqrt{2}}(p_z^t - p_z^b), \tag{3}$$

where t and b imply to the top and bottom P orbitals respectively. p^t and p^b refer to symmetric and antisymmetric of p orbitals respectively. The even subspace of d orbitals of the Tungsten atom is also $(d_{xy}, d_{x^2-y^2}, d_{3z^2-r^2})$. Eventually, the Hilbert space in even subspace for WSe_2 monolayer is $(d_{xy}, d_{x^2-y^2}, d_{3z^2-r^2}, P_x^S, P_y^S, P_z^A)$. (more details is in ref [8]). Based on this descriptions, the six-band Hamiltonian in real space can be explained as:

$$H^{TB} = \sum_{i.\mu\nu} \in_{\mu\nu} c_{i.\mu}^{\dagger} c_{i.\nu} + \sum_{ij.\mu\nu} [t_{ij.\mu\nu} c_{i.\mu}^{\dagger} c_{j.\nu} + H.C], \tag{4}$$

where, $c_{i.\mu}^{\dagger}$ create an electron in the unit cell i in the atomic orbital μ. Also $\in$ and t denote onsite and hopping energies respectively. Using Fourier transformation, the six-band Hamiltonian in real space (Eq. (4)), can be transformed to the k space as following:

$$H^{TB}(k) = \varepsilon + \sum_{i=1}^{3} \begin{bmatrix} 2t_i^{MM}\cos(k\cdot v_i) & t_i^{MX} e^{-ik\cdot u_i} \\ t_i^{XM} e^{ik\cdot u_i} & 2t_i^{XX}\cos(k\cdot v_i) \end{bmatrix}, \tag{5}$$

where $\varepsilon = \mathrm{diag}(\varepsilon_M, \varepsilon_X)$ are onsite energy matrices, u and v denote nearest and next nearest neighbors respectively, (see Fig. 1). Moreover M and X refer to W and Se atoms, respectively. It should be mentioned that distance between nearest neighbor in plane W-W and Se-Se is 3.26 A^0 and the out of plane bound length of W-Se is 2.21 A^0 [14].

Tight binding parameter including crystal fields f_α and hopping terms V_α of the WSe_2 single-layer are calculated by fitting the low energy of conduction and valence bands [8], and the results are provided in Table 1. It should be noted that the crystal fields f_0, f_1, f_2 refer to the atomic levels of the Tungsten orbitals consist of $l = 0\,(d_{3z^2-r^2})$, $l = 1(d_{xz}, d_{yz})$ and $l = 2(d_{xy}, d_{x^2-y^2})$ respectively. Due to d_{xz}, d_{yz} orbitals are not involved in six-band model, the f_1 is not included in Table 1. Also f_p and f_z denote the atomic level of the in-plane p_x, p_y and out-of-plane p_z of the Selenium atom respectively. By using these parameters, the hopping and onsite energies of WSe_2 single-layer for six-band tight binding model have been calculated using and results are provided in Appendix A. To obtain the Hamiltonian in the k space for WSe_2 nanoribbon, the Fourier transformation of Eq. (4) must be only in one direction. Therefore, the Hamiltonian of WSe_2 nanoribbons in k space can be written as following:

$$H = H_{00} + e^{ika}H_{-10} + e^{-ika}H_{-10}^{\dagger}, \tag{6}$$

where H_{00} is Hamiltonian of a unit cell indicated in Fig. 1(a), and H_{-10} is the Hamiltonian between H_{00} and its adjacent unit cell. Notice that we consider n = 36 and n = 38 atoms for armchair and zigzag WSe_2 nanoribbons unite cell, respectively. So, the ribbon width for armchair and zigzag WSe_2 nanoribbons are 29.34 A^0 and 49.27 A^0, respectively.

3. Green's function method

Quantum transport parameters of nanoribbons provide us information about electric current along the ribbon direction and also the number of channels of the electric current. The system that is considered to investigate the electronic transport is a WSe_2 nanoribbon. In order to calculate the conductance of WSe_2 nanoribbons, we use the non-equilibrium Green's function method (NEGF) which have been extended by Lopez et al. [15]. In this method, ribbon is divided to three